LOOP ALGORITHMS FOR DUCTILITY ANALYSIS OF COLUMN REINFORCED STEEL WITH YIELD STRENGTH ABOVE 500 MPA

[1]AHMAD FAZA AZMI

[1]East Java Regional Residential Infrastructure Center, Directorate General Of Copyright Works,

Minister for Public Works and Human Settlements

e-mail: [1]faza.azmi@pu.go.id

ABSTRACT

There are many benefits to the use of high-strength reinforcement (above 500 MPa) in reinforced concrete buildings. The advantages of using high-strength reinforcement are reduction steel volume and dimension, reduced construction time, reduction in reinforcement congestion, as well as savings in materials and worker cost. Meanwhile, the investigation of ductility of reinforced concrete element with high-strength reinforcement to resist earthquake effects under current design procedure is needed. In the current standard, ACI 318-71, The maximum specified yield strength was restricted to 60 Ksi (413 MPa) for reinforcement in special seismic system. There were also no ASTM standard specifications for reinforcement with yield strength above 500 MPa. In the design of seismic resisting structures, the analysis of curavture ductility and flexural overstrength factor is of important consideration in order to avoid brittle failure. This paper attempts to anaylze the ductility and re-evaluate the flexural overstrength factor of reinforced concrete column. The tensile tests of steel reinforcement with yield strength above 500 MPa generates stress-strain curve. An idealisations for the monotonic stress-strain curve proposed by mander was adopted in this study. Whereas in this numerical study of confined concrete columns, the behavior of concrete cored is modeled by the stress-strain relationship of confined concrete proposed by Kappos-Konstantinidis. This stress strain model was used for the momen, curvature, ductility, and flexural overstrength factor analysis.

Keywords: *Column, Steel, Ductility, Flexural, Overstrengthfactor*

1. INTRODUCTION

There are many potential advantages to the use of high-strength reinforcement (above 500 MPa) in reinforced concrete structures. There are reduction steel volume, reduced construction time, reduction in reinforcement congestion,as well as savings in material and worker cost. Meanwhile, the investigation of ductility of reinforced concrete element with high-strength reinforcement to resist earthquake effects under current design procedure is needed. In the current standard, ACI 318-71, The maximum specified yield strength was restricted to 60 Ksi (413 MPa) for reinforcement in special seismic system. There were also no ASTM standard specifications for reinforcement with yield strength above 500 MPa.

This paper attempts to analyse the ductility and re-evaluate the flexural overstrength factor of reinforced conrete column. The stress-strain model proposed by mander has six key paramaters. The six key parameters, which are used to form the stress-strain curve, are obtained from the tensile tests, there are f_y,ε_y,E_s,f_sh,ε_sh,E_sh . The number of the samples tested is 78 specimen and the mean value of the six key parameters are listed in Table 2.

2. STEEL REINFORCEMENT MODELS

Previous investigations have shown that the plastic hinge behavior of reinforced concrete members is determined by the stress strain curve of the reinforcing steel (Park, 1977). The tensile tests are necessary to determine the stress strain characteristic of the reinforcing steel . The tensile tests generate stress-strain curve of the steel bars with yield strength above 500 MPa. The stress-strain curve of the steel bars, obtained from tensile tests, approach the stress-strain curve proposed by mander.

Based on the stress-strain properties of reinforcing steel, theoretical curvature ductilty, and overstrength factor analyses are carried out for reinforced concrete column.
Curvature ductility and flexural overstrength factor analysis was calculated using numerical analysis by using loop algorithms.
Numerical analysis can be used to simulate the behavior of reinforced concrete columns by entering the strain values into the given formula (function) so as to produce stress and internal forces values in the reinforced concrete column.
For this numerical analysis to be performed, a function (formula) which represents the relationship betweeen stress and strain (steel and concrete) in a reinforced concrete element is required. While on the steel tensile test, it only produces stress-strain curve of steel without the function (formula) that forms the stress-strain curve of the steel bars.
Due to the above problems, this study adopts the stress-strain curve of the steel bars proposed by Mander so that the strain value can be entered into numerical analysis by computer program (VBA Macro Excel) so that the value of stress and internal forces in the reinforced concrete column can be obtained. Furthermore, the stress-strain curve of the steel bars proposed by Mander is considered to represent the stress-strain curve of tensile test results.
The stress-strain curve of the steel bars, proposed by Mander, is calculated using the following equation.

a. Linear Elastic $\left(0 \le \varepsilon_s \le \varepsilon_y\right)$

$$f_s = E_t \varepsilon_s \quad (1)$$

$$E_t = E_s \quad (2)$$

$$\varepsilon_y = f_s / E_s \quad (3)$$

E_t = tangen modulus

E_s = modulus of elasticity of the steel (Young's modulus)

b. Yield Plateau $\left(\varepsilon_y < \varepsilon_s \le \varepsilon_{sh}\right)$

$$f_s = f_y, E_t = 0 \quad (4)$$

c. Strain Hardening $\left(\varepsilon_{sh} < \varepsilon_s \le \varepsilon_{su}\right)$

Strain that occurs is followed by the increased value of f_s exceed f_y and continue until the ultimate strain $\left(\varepsilon_{su}\right)$ is reached. At point D maximum stress is reached. The expression for the strain hardening area is in the form of a power curve, with the ultimate stress-strain coordinate as origin, as follows :

$$\left[\frac{f_{su} - f_s}{f_{su} - f_y}\right] = \left[\frac{\varepsilon_{su} - \varepsilon_s}{\varepsilon_{su} - \varepsilon_{sh}}\right]^P \quad (5)$$

$$f_s = f_{su} + \left(f_y - f_{su}\right)\left|\frac{\varepsilon_{su} - \varepsilon_s}{\varepsilon_{su} - \varepsilon_{sh}}\right|^P \quad (6)$$

Where P is the strain hardening power and can be determined by differentiating Equation 6 to give the tangent modulus :

$$E_t = \frac{df_s}{d\varepsilon_s} = P\left[\frac{f_{su} - f_y}{\varepsilon_{su} - \varepsilon_{sh}}\right]\left|\frac{\varepsilon_{su} - \varepsilon_s}{\varepsilon_{su} - \varepsilon_{sh}}\right|^{P-1} \quad (7)$$

Since the strain hardening modulus $\left(E_{sh}\right)$ occurs when $\varepsilon_s = \varepsilon_{sh}$,therefore :

$$E_t = E_{sh} = P\left[\frac{f_{su} - f_y}{\varepsilon_{su} - \varepsilon_{sh}}\right] \text{ atau} \quad (8)$$

$$P = E_{sh}\left[\frac{\varepsilon_{su} - \varepsilon_{sh}}{f_{su} - f_y}\right] \quad (9)$$

Stress at yield point (point B in figure 1) is considered as yield strength, and used as parameter in elastic design of steel reinforcement. The modulus of elasticity average values (Es) is deternined by the slope of the linear static. Which is generally determined as 200 GPa, however, from the tensile tests, the modulus of elasticity average values is 212288 MPa.
The comparison stress-strain value that is obtained from tensile tests and The stress-strain value that is obtained from mander formula is shown in Table 1.

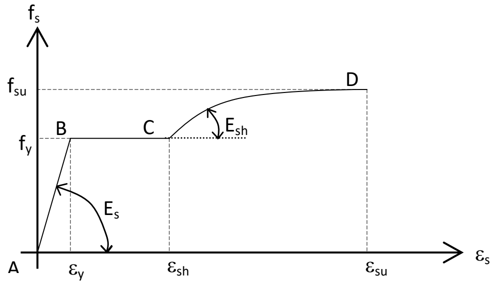

Figure 1. Stress-strain curve of steel (Mander et al, 1984)

The stress-strain value of the reinforcing steel proposed by Mander is shown in Table 1. It can be obtained from the mean values of stress and strain of reinforcing steel at yield, initial strain hardening, and ultimate strain hardening which are shown in Table 2 (Result and Discussion section), by inputting the value of strain into equation (1) to equation (9). Then the strain value is increased by certain increment.

The stress-strain value of the reinfrocing steel obtained from tensile test results also shown in Table 1. It is obtained from the mean values of stress-strain test specimen.

In Figure 2, the stress-strain curve shows an explicitly upper yield strenght point. The upper yield strength value, from tensile tests, as shown in Table 1, is 526.87 MPa. The relative magnitude of the upper yield point depends on the speed of testing, the shape of the section and the form of the specimen (Park and Paulay, 1975).

Table 1. Stress strain of steel from the tensile test (MPa)

Condition	Mander		Tensile Test	
	Strain	Stress	Strain	Stress
Yield	0.002441	518.1224	0.002441	518.1224
Yield Plateau	0.005383	518.1224	0.005383	526.8793
	0.008325	518.1224	0.008325	528.1957
	0.011267	518.1224	0.011267	528.6989
	0.014209	518.1224	0.014209	529.3922
Strain hardening	0.017151	518.1224	0.017151	530.5282
	0.029513	549.6992	0.029513	570.127
	0.041874	577.5556	0.041874	598.9098
	0.054235	601.7469	0.054235	621.9042
	0.066597	622.3352	0.066597	640.6962
	0.078958	639.3906	0.078958	653.4712
	0.09132	652.9946	0.09132	662.4942
	0.103681	663.2444	0.103681	668.877
	0.116042	670.2621	0.116042	672.487
	0.128404	674.2146	0.128404	674.384
Ultimate	0.140765	675.3878	0.140765	675.3878

The yield plateau length (B-C in Figure 1) is generally function of the strength of the steel. From monotonic tension tests, the stress value at yield plateau region is between 526,87 to 530,52 MPa whereas the stress value obtained from mander formula clasically treated as flat and with zero tangent modulus as shown in Figure 2, the stress obtained from mander formula remains constant while the strain continues to increase. It caused the difference value of stress between stress-strain curve proposed by mander with stress-strain curve obtained from monotonic tension test although not significant. The ultimate stress occurs at Point D in Figure 1. This point is assumed as the ultimate strain rather than the fracture strain which occurs at a lower stress and higher strain. The comparison between stress- strain curve of reinforcing steel obtained from monotonic tension tests and mander formula is shown Figure 2.

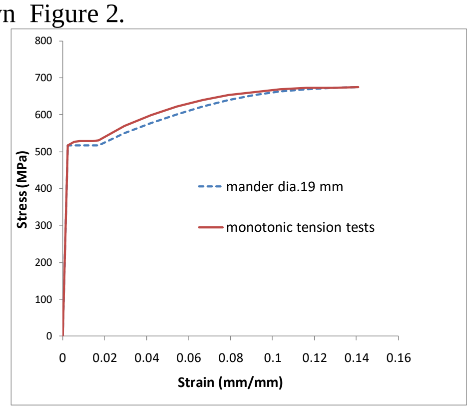

Figure 2. Comparisons Stress-Strain Curve of Reinforcing Steel between monotonic tension tests and mander

3. CONFINED CONCRETE MODELS

The stress-strain model proposed by Kappos-Konstantinidis for confined concrete under monotonic compressive loading was adopted. The comparison of stress-strain model between confined concrete (Kappos-Konstantinidis) and unconfined concrete (Kent-Park) shown in Figure 3. The definiton of ultimate strain assumed at which ultimate stress occurs, rather than at fracture point which occurs at a lower stress. Confinement in addition to increasing stress and strain of concrete, also to avoid over-reinforced condition on reinforced concrete columns. It is necessary for the steel to be able to undergo large plastic strains before the concrete reaches the ultimate strain.

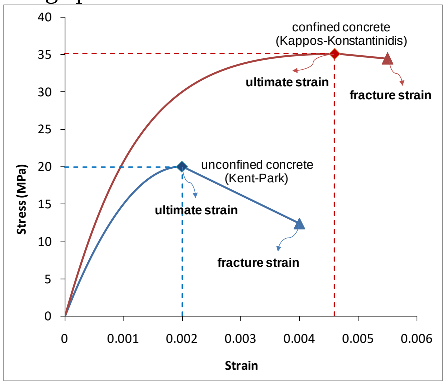

Figure 3. Confined and Unconfined Stress-Strain Curve of Concrete

4. MOMENT, CURVATURE, DUCTILITY AND OVERSTRENGTH FACTOR ANALYSES

The curvature of a member is defined as the rotation per unit length. The moment-curvature curve for a reinforced concrete section can be traced theoretically using the requirements of strain compatibility and equilibrium of internal forces (Park and Paulay, 1975).

The analysis start from εcm = 0.000005. and then loop algorithms gradually increasing the εcm value by increments of 0.000005. For each value of εcm the neutral axis depth (kd) is adjusted and the internal forces in the concrete and the steel is found. When the internal forces is found, the moment M and curvature is found.

5. RESULT AND DISCUSSION

When The stress-strain properties of reinforcing steel obtained from a monotonic tension test as used for longitudinal reinforcement shown in Table 2. There are 30 models with various reinforced concrete column properties which are used as models in this investigation. The data value for some models of the specimen to be analyzed, can be seen in Table 3.

The moment-curvature relationship is shown in Figure 4. Figure 4 exhibit a discontinuity at first yield of the tension steel and have been terminated when the steel strain reaches strain hardening ultimate (εshu is assumed as εsu). Figure 4 indicate the ductility of the section is sigficantly reduced by the presence of axial load.

Table 2. Steel properties from the tensile test (MPa)

Diameter of Bars 19 mm			
	f_y	f_{sh}	$f_{sh\ ult}$
Mean	518.1224	530.5282	675.3878
	ε_y	ε_{sh}	$\varepsilon_{sh\ ult}$
Mean	0.002441	0.017151	0.140765
Total of Samples		38	
Diameter of Bars 22 mm			
	f_y	f_{sh}	$f_{sh\ ult}$
Mean	503.6793	514.2421	665.0723
	ε_y	ε_{sh}	$\varepsilon_{sh\ ult}$
Mean	0.002478	0.016764	0.136128
Total of Samples		40	

Table 3. Section properties of column models

No	A (mm)	B (mm)	C (MPa)	D	E	F	G (mm)	H (MPa)	I (mm)
1									320x320
2						D19	100	300	400x400
3									500x500
4									320x320
5						D22	100	300	400x400
6									500x500
7				2	2		50		
8						D19	100	300	400x400
9							150		
10							200		
11							50		
12						D22	100	300	400x400
13							150		
14	10	40	20				200		
15				2	2				
16				3	3	D19			
17				4	4		100	300	400x400
18				2	2				
19				3	3	D22			
20				4	4				
21								200	
22				2	2	D19	100	300	400x400
23								400	
24								500	
25								200	
26				2	2	D22	100	300	400x400
27								400	
28								500	
29	10	40	30	2	2	D19	100	300	400x400
30						D22			

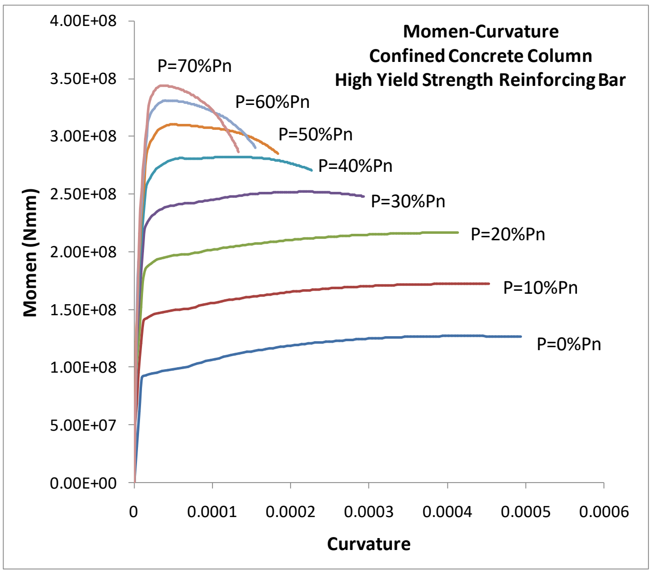

Figure 4. Effect of Axial Load on Moment-Curvature Curve

Table 4 reveal the influence of column area on the column flexural overstrength factor and curvature ductility. Table 5 reveal the influence of transverse reinforcement spacing on the column flexural overstrength factor and curvature ductility. Table 5 reveal the influence of reinforcement ratio on the column flexural overstrength factor and curvature ductility. Table 5 show the effect of transverse bar yield strength on the column flexural overstrength factor and curvature ductility. Table 6 show the effect of concrete compression strength on the column flexural overstrength factor and curvature ductility.

Table 4. Curvature ductility and overstrength factor of column model 1-6

No	width x depth	P/Pn	μφ mean	λ0 mean	No	width x depth	P/Pn	μφ mean	λ0 mean
1	320x320 mm	0%	27.59774	1.205021	4	320x320 mm	0%	22.61007	1.199156
		10%	20.9468	1.142588			10%	18.38696	1.152273
		20%	16.82654	1.145527			20%	15.05599	1.167069
		30%	11.16828	1.252914			30%	9.83067	1.318216
		40%	8.113128	1.45598			40%	7.939746	1.525626
		50%	7.349483	1.658709			50%	7.250162	1.727583
		60%	6.965344	1.899888			60%	6.848009	1.727583
		70%	6.743569	2.267675			70%	6.617517	2.30286
2	400x400 mm	0%	38.82601	1.239789	5	400x400 mm	0%	27.98066	1.234346
		10%	25.40629	1.141497			10%	23.81144	1.153754
		20%	19.37351	1.131233			20%	16.88271	1.143172
		30%	11.9714	1.159874			30%	10.66488	1.178537
		40%	8.174235	1.3268			40%	7.736116	1.368689
		50%	7.242987	1.516635			50%	7.171104	1.558718
		60%	6.963187	1.743437			60%	6.866014	1.783941
		70%	6.807308	2.086627			70%	6.697082	2.122766
3	500x500 mm	0%	44.57443	1.270774	6	500x500 mm	0%	38.12032	1.267146
		10%	33.17002	1.131175			10%	27.3468	1.146506
		20%	19.08353	1.108993			20%	17.5314	1.118084
		30%	11.57543	1.135569			30%	10.82738	1.136498
		40%	7.910262	1.248385			40%	7.559381	1.270044
		50%	7.12519	1.423261			50%	7.099014	1.448317
		60%	6.943154	1.631732			60%	6.891836	1.659066
		70%	6.846582	1.943816			70%	6.78232	1.970891

Table 5. Curvature ductility and overstrength factor of column model 7 - 28

No	P/Pn	μφ mean	λ0 mean	No	P/Pn	μφ mean	λ0 mean
7	0%	68.155	1.349	9	0%	26.012	1.161
	10%	49.933	1.228		10%	16.198	1.083
	20%	40.183	1.217		20%	11.971	1.08
	30%	24.907	1.242		30%	7.6062	1.123
	40%	17.561	1.406		40%	6.7602	1.276
	50%	12.701	1.632		50%	6.4356	1.437
	60%	9.6849	1.926		60%	6.2756	1.614
	70%	7.4032	2.383		70%	6.1971	1.833
8	0%	38.826	1.24	10	0%	19	1.108
	10%	25.406	1.141		10%	11.196	1.045
	20%	19.374	1.131		20%	7.7571	1.051
	30%	11.971	1.16		30%	5.2029	1.093
	40%	8.1742	1.327		40%	4.7337	1.23
	50%	7.243	1.517		50%	4.5157	1.367
	60%	6.9632	1.743		60%	4.4104	1.464
	70%	6.8073	2.087		70%	4.4781	1.617
No	P/Pn	μφ mean	λ0 mean	No	P/Pn	μφ mean	λ0 mean
11	0%	52.836	1.347	13	0%	18.527	1.151
	10%	45.725	1.25		10%	14.976	1.088
	20%	35.055	1.242		20%	10.592	1.089
	30%	22.361	1.271		30%	7.4269	1.142
	40%	15.75	1.453		40%	6.7035	1.317
	50%	11.624	1.678		50%	6.3509	1.477
	60%	8.7797	1.974		60%	6.1776	1.642
	70%	6.6155	2.436		70%	6.1422	1.834
12	0%	27.981	1.234	14	0%	13.821	1.097
	10%	23.811	1.154		10%	10.436	1.046
	20%	16.883	1.143		20%	7.0705	1.052
	30%	10.665	1.179		30%	5.3328	1.113
	40%	7.7361	1.369		40%	4.8132	1.269
	50%	7.1711	1.559		50%	4.5706	1.401
	60%	6.866	1.784		60%	4.4591	1.47
	70%	6.6971	2.123		70%	4.6353	1.616

No	longitudinal steel Ast (mm^2)	ρ	P/Pn	μφ mean	λ0 mean
15	1134.114948	0.0071	0%	38.82601	1.239789
			10%	25.40629	1.141497
			20%	19.37351	1.131233
			30%	11.9714	1.159874
			40%	8.174235	1.3268
			50%	7.242987	1.516635
			60%	6.963187	1.743437
			70%	6.807308	2.086627
16	1701.172422	0.0106	0%	29.64941	1.217909
			10%	23.70118	1.152181
			20%	16.96006	1.138542
			30%	10.48851	1.183428
			40%	7.798096	1.374991
			50%	7.221359	1.570685
			60%	6.895314	1.801419
			70%	6.714223	2.141861
17	2268.229896	0.0142	0%	27.96766	1.209665
			10%	21.94859	1.161595
			20%	14.93177	1.138372
			30%	9.485997	1.218864
			40%	7.781492	1.416571
			50%	7.154041	1.613011
			60%	6.80422	1.842079
			70%	6.611503	2.162602
No	longitudinal steel Ast (mm^2)	ρ	P/Pn	μφ mean	λ0 mean
18	1520.530844	0.0095	0%	27.98066	1.234346
			10%	23.81144	1.153754
			20%	16.88271	1.143172
			30%	10.66488	1.178537
			40%	7.736116	1.368689
			50%	7.171104	1.558718
			60%	6.866014	1.558718
			70%	6.697082	2.122766
19	2280.796267	0.0143	0%	26.40738	1.218033
			10%	21.09245	1.165615
			20%	14.41464	1.145421
			30%	9.228261	1.230005
			40%	7.679353	1.42741
			50%	7.06787	1.618559
			60%	6.728633	1.84199
			70%	6.542099	2.156825
20	3041.061689	0.019	0%	24.58078	1.213057
			10%	19.14955	1.175988
			20%	12.79452	1.14499
			30%	8.658114	1.279141
			40%	7.565983	1.473554
			50%	6.925558	1.660571
			60%	6.574899	1.87273
			70%	6.588596	2.128932

No	P/Pn	μφ mean	λ0 mean	No	P/Pn	μφ mean	λ0 mean
21	0%	29.25	1.185	23	0%	47.319	1.279
	10%	18.492	1.1		10%	31.318	1.172
	20%	13.924	1.096		20%	24.415	1.159
	30%	8.4853	1.135		30%	15.256	1.183
	40%	6.4889	1.293		40%	10.361	1.35
	50%	6.1153	1.464		50%	8.0696	1.554
	60%	5.9204	1.66		60%	7.6903	1.803
	70%	5.8179	1.931		70%	7.4848	2.183
22	0%	38.826	1.24	24	0%	54.818	1.307
	10%	25.406	1.141		10%	37.272	1.195
	20%	19.374	1.131		20%	29.276	1.182
	30%	11.971	1.16		30%	18.487	1.203
	40%	8.1742	1.327		40%	12.482	1.368
	50%	7.243	1.517		50%	9.0923	1.583
	60%	6.9632	1.743		60%	7.4018	1.849
	70%	6.8073	2.087		70%	7.1083	2.258
No	P/Pn	μφ mean	λ0 mean	No	P/Pn	μφ mean	λ0 mean
25	0%	21.583	1.177	27	0%	34.294	1.277
	10%	17.617	1.108		10%	29.603	1.189
	20%	12.49	1.106		20%	21.292	1.173
	30%	7.7086	1.153		30%	13.535	1.203
	40%	6.5412	1.334		40%	9.3148	1.392
	50%	6.1296	1.504		50%	7.9727	1.597
	60%	5.915	1.694		60%	7.5903	1.846
	70%	5.8028	1.939		70%	7.3664	2.226
26	0%	27.981	1.234	28	0%	40.69	1.307
	10%	23.811	1.154		10%	35.027	1.215
	20%	16.883	1.143		20%	25.699	1.199
	30%	10.665	1.179		30%	16.415	1.226
	40%	7.7361	1.369		40%	11.417	1.411
	50%	7.1711	1.559		50%	8.3169	1.627
	60%	6.866	1.784		60%	7.3229	1.894
	70%	6.6971	2.123		70%	7.0475	2.305

Table 6. Curvature ductility and overstrength factor of column model 29, 30

No	P/Pn	μφ mean	λ0 mean
29	0%	31.87612	1.206455
	10%	20.25377	1.086586
	20%	13.79796	1.073527
	30%	8.355373	1.108279
	40%	5.988974	1.218472
	50%	5.712133	1.356078
	60%	5.574538	1.503026
	70%	5.506238	1.69581
No	P/Pn	μφ mean	λ0 mean
30	0%	26.89537	1.195343
	10%	19.0761	1.094898
	20%	12.83532	1.083489
	30%	7.670564	1.112439
	40%	6.059716	1.247438
	50%	5.743641	1.386436
	60%	5.585848	1.528571
	70%	5.50762	1.704156

6. CONCLUSIONS

The overstrength value decreased at low levels of axial load (P/Pn 0% - 30%) but at higher axial loads (P/Pn > 30%), the ratio of Mmax (experimental flexural strengths of square columns section) to Mi (predictions based on ideal flexural strenght) increased as shown by Tables 4, 5, 6, 7, and 8. The Ideal flexural strength is determined by using measured material strengths, an ultimate compression strain of 0.003. The increase in compression zone depth, kd, with axial load, and hence the greater importance of the term Cc (kd – β.kd/2) to the total flexural strength caused the increased of overstrength factor.

The relationship between axial load and The curvature ductility (μφ) is obtained from Tables 4, 5, 6, 7, and 8. It is exhibit that the ductility of the column is significantly reduced by the presence of axial load. The flexural overstrength value for column reinforced steel with yield strength above 500 MPa is 1.04 – 2.30.

The stress-strain curve for high strength reinforcement can be determined by six variable basic parameters ($f_y, \varepsilon_y, E_s, f_{sh}, \varepsilon_{sh}, E_{sh}$).

There are six key parameters (column area, transverse reinforcement spacing, reinforcement ratio, transverse bars yield strength, concrete compression strength, and axial load) primarily influence the curvature ductility and flexural overstrength factor. The most influencing parameter is found to be the presence of axial load

REFRENCES

[1]. ACI, 2011, Building Code Requirements for Structural Concrete and Commentary, ACI 318-11, ACI Committee 318, American Concrete Institute, Farmington Hills, Michigan.

[2]. Andriono, T., and Park, R., (1986), “Seismic Design Considerations of the Properties of New Zealand Manufactured Steel Reinforcing Bars”, Bulletin of the New Zealand National Society for Earthquake Engineering, Vol.19, No. 3, September 1986 [3] Todd, K.D. and Mays, L.W. (2005). *Groundwater Hydrology*, 3rd edition, John Wiley & Sons, Inc., New York.

[3]. Andriono, T., (1986), Properties of Reinforcing Steel Used In Seismic Design, Report submitted in partial fulfilment of the Requirments for the Degre of Master of Engineering at the University of Canterbury

[4]. ASTM, 2009a, Standard Specification for Deformed and Plain Carbon-Steel Bars for Concrete Reinforcement, ASTM A615-09b, ASTM International, West Conshohocken, Pennsylvania.

[5]. ASTM, 2009a, Standard Specification for Deformed and Plain Carbon-Steel Bars for Concrete Reinforcement, ASTM A615-09b, ASTM International, West Conshohocken, Pennsylvania.

[6]. ASTM, 2009b, Standard Specification for Low-Alloy Steel Deformed and Plain Bars for Concrete Reinforcement, ASTM A706-09b, ASTM International, West Conshohocken, Pennsylvania.

[7]. Lim Wai Tat (1991), Statistical Analysis of Reinforcing Steel Properties, University of Canterbury Christchurch, New Zealand.

[8]. Kent, D. C., and Park, R., Flexural Members with Confined Concrete, Journal of Structural Division, ASCE, V. 97, No. ST7, July 1971, pp. 1969-1990.

[9]. Kappos, A. J., and Konstantinidis, D., Statistical Analysis of Confined High-Strength Concrete Columns, Material and Structures, V. 32, Dec. 1992, pp. 734-748.

[10]. Mander, J. B., Priestley, M. J. N., and Park, R. (1984). "Seismic design of bridge piers." Research Rep. 84-02, Dept. of Civ. Engrg., University of Canterbury, Christchurch, New Zealand.

[11]. Park. R; Paulay. T (1975), Reinforced Concrete Structures, John Wiley and Sons, New York, USA

[12]. Park, R., "Constitutive Relations of Steel : Effect on Strength Consideration in Seismic Design", Proceedings of Workshop on Earthquake Resistant Reinforced Concrete Building Construction, Vol.II, University of California, Berkeley, July 1977, pp. 683-695

[13]. Priestley, M.J.N; Paulay,T (1990), Seismic Design of Reinforced Concrete and Masonry Buildings, John Wiley and Sons, , 3rd edition.

[14]. Standar Nasional Indonesia 03-1726-2002, Tata Cara Perencanaan KetahananGempa untuk Bangunan Gedung, Badan Standardisasi Nasional , Jakarta.

[15]. Standar Nasional Indonesia.SNI-03-2847-2002 - Tata Cara Perhitungan Struktur Beton Untuk Bangunan Gedung, Standar Nasional Indonesia.

[16]. Susanti Eka (2012), "Kemampuan Daktilitas Baja Tulangan Dengan Mutu Diatas 400 MPa Untuk Disain Struktur Tahan Gempa", Seminar Nasional Pascasarjana XII - ITS, Surabaya.